nature photonics

REVIEW ARTICLE

PUBLISHED ONLINE: 29 SEPTEMBER 2016 | DOI: 10.1038/NPHOTON.2016.186

Solid-state single-photon emitters

Igor Aharonovich[1,2]*, Dirk Englund[3] and Milos Toth[1,2]

Single-photon emitters play an important role in many leading quantum technologies. There is still no 'ideal' on-demand single-photon emitter, but a plethora of promising material systems have been developed, and several have transitioned from proof-of-concept to engineering efforts with steadily improving performance. Here, we review recent progress in the race towards true single-photon emitters required for a range of quantum information processing applications. We focus on solid-state systems including quantum dots, defects in solids, two-dimensional hosts and carbon nanotubes, as these are well positioned to benefit from recent breakthroughs in nanofabrication and materials growth techniques. We consider the main challenges and key advantages of each platform, with a focus on scalable on-chip integration and fabrication of identical sources on photonic circuits.

Photonic technologies are becoming increasingly prevalent in our daily lives. After decades of rapid advances, light sources — especially lasers and light-emitting diodes — have become high-performance, yet low-cost and reliable components, driving the Internet and lighting cities. A new frontier of research is the development of non-classical light sources: sources that produce streams of photons with controllable quantum correlations. A central building block, in particular, is a single-photon emitter (SPE) — a fundamental resource for many scalable quantum information technologies[1–6]. The ideal on-demand SPE emits exactly one photon at a time into a given spatiotemporal mode, and all photons are identical so that if any two are sent through separate arms of a beam-splitter, they produce full interference (a signature of indistinguishability). Such SPEs play a central role in a range of proposed quantum computing schemes, including linear[7,8] quantum simulation[9], quantum walks[10] and boson sampling[11], and precision measurement[12]. SPEs are also useful or necessary in many quantum secure communication schemes[13,14] and light flux metrology applications (such as defining the quantum candela — the SI base unit of luminous intensity) that do not require indistinguishability[15,16].

Over the years, various processes have been studied to generate single photons. The first demonstration of a SPE used an atomic transition of sodium atoms[17], though its reliability and efficiency were low. Today, it is possible to control cold atoms to efficiently produce single photons on-demand with near-identical wave packets[18]. Such sources, however, still require complex set-ups, and the loading of atoms or ions can be intermittent. The dynamics of atom-based sources is also relatively slow, leading to very low operation rates. Alternatively, single photons can be generated by heralding one of two photons produced using a nonlinear process such as spontaneous parametric down-conversion[19,20] or spontaneous four-wave mixing[21]. To overcome the unpredictable generation times of heralded photons, multiplexing schemes are being developed to rearrange them into regular intervals, though more work is needed to improve the single-photon purity and efficiency of such schemes, which are currently limited largely by losses in switching, photon storage and detection.

One of the most promising types of single-photon sources today are solid-state SPEs based on atom-like emitters — including fluorescent atomic defects and quantum dots (QDs) — which promise to combine the outstanding optical properties of atoms with the convenience and scalability of a solid-state host system[22–25]. But the complex mesoscopic environment of the solid state also entails numerous challenges, including inhomogeneous distributions that cause variability between photons from different emitters, and homogeneous linewidth broadening that gives rise to photon distinguishability from the same emitter. In addition, the extraction of photons, particularly from emitters in host materials with high refractive index, is challenging. Much research over the past decade has focused on mitigating these deleterious effects.

Over the past decade, efforts to engineer solid-state SPEs have expanded beyond the originally studied colour centres and QDs to include two-dimensional (2D) materials, carbon nanotubes (CNTs) and other solid-state host materials. A range of other source technologies are transitioning from discovery into engineering. This Review will identify key properties for evaluating and comparing SPEs, and will summarize recent progress of 'established' and emerging SPE technologies. In particular, we discuss the SPEs' photophysical properties as well as efforts towards scalable system integration, including electrical triggering and incorporation into optical resonators (metallic and dielectric).

We will first briefly review the available and most-studied solid-state systems, summarized in Fig. 1, and consider leading sources and their photophysical properties. We will then discuss important steps towards engineering scalable devices based on solid-state sources, with an emphasis on electrically triggered sources and integration of emitters with optical resonators (metallic and dielectric). We conclude with a discussion of challenges inherent to each system and highlight new research directions that are currently being explored.

Table 1 summarizes some of the most important properties of each system and serves as a roadmap for future studies of each system. It is clear that no single platform satisfies all prerequisites for an ideal SPE. For most applications, stable SPEs (which do not blink or bleach) are needed, with a high brightness and emission rate, as well as high single-photon purity and indistinguishability. The brightness of the source represents the maximum rate at which single photons can be emitted (or collected), while purity characterizes the multiphoton emission probability. Purity is quantified

[1]School of Mathematical and Physical Sciences, University of Technology Sydney, Ultimo, New South Wales 2007, Australia. [2]Institute for Biomedical Materials and Devices (IBMD), Faculty of Science, University of Technology Sydney, New South Wales 2007, Australia. [3]Department of Electrical Engineering and Computer Science, Massachusetts Institute of Technology, Cambridge, Massachusetts 02139, USA.
*e-mail: igor.aharonovich@uts.edu.au

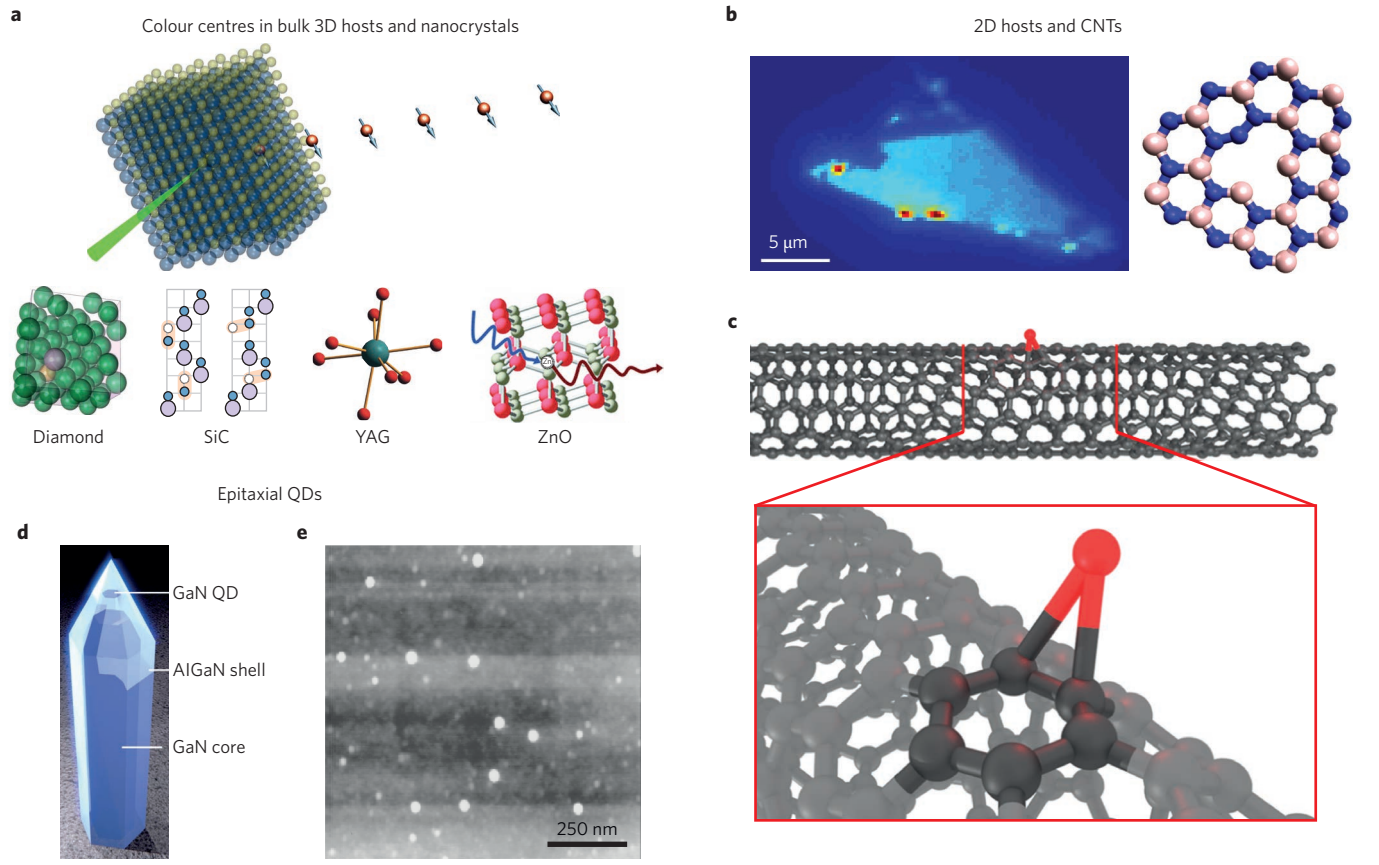

Figure 1 | Solid-state quantum systems emphasized in this Review. a, Defects in bulk 3D crystals and nanocrystals that emit single photons when excited with sub-bandgap light (illustrated with a green incoming laser beam). The insets show the most studied crystals — diamond, silicon carbide (SiC), yttrium aluminium garnet (YAG) and zinc oxide (ZnO). **b**, Emitters in 2D hosts. Single-photon emission at cryogenic temperatures was realized from localized excitons in several TMDCs including WSe_2 and $MoSe_2$, as shown in the confocal map (left). Room-temperature operation was realized from defects in monolayer hBN and few-layer flakes of hBN (right). **c**, Single-photon emission was recorded from excitons localized at oxygen-related defects in single-walled CNTs. **d**, Nitride QD embedded in a nanowire waveguide in order to enhance emission. **e**, Self-assembled InAs QDs. Both QD systems are representative of epitaxial (non-colloidal) QD-based SPE platforms. The InAs QDs were the first system used to demonstrate triggered SPEs. Figure reproduced with permission from: **a**(SiC), ref. 35, Nature Publishing Group; **a**(YAG), ref. 49, Nature Publishing Group; **a**(ZnO), ref. 44, American Chemical Society; **b**(left), ref. 61, OSA; **b**(right), ref. 56, Nature Publishing Group; **c**, ref. 68, Nature Publishing Group; **d**, ref. 85, American Chemical Society; **e**, ref. 74, APS.

by the dip of the second-order autocorrelation function, $g^{(2)}(\tau)$, at zero delay time, τ, while photon indistinguishability is quantified by a corresponding dip in the Hong–Ou–Mandel two-photon interference experiment that measures the extent of destructive interference between photons arriving simultaneously at a 50:50 beam splitter. These quantities are not consistently available, especially not under comparable experimental conditions (for example pump power) and especially not for emerging SPE systems. As the field of SPEs matures, it will become important to adopt consistent measurement and reporting standards to aid comparisons between SPE systems and for informing theoretical protocols. For the purpose of this Review, we have assembled the arguably most consistently reported SPE metrics in Table 1.

So far, only InGaAs QDs offer purities in excess of 99% (whereby $g^{(2)}(0) < 0.01$), corresponding to a 100-fold reduction in multiphoton emission compared with single-photon emission[24–27]. Most other systems suffer from increased multiphoton emission events with $g^{(2)}(0)$ in the range of 0.1–0.3, although many have very high emission rates of the order of 10^6 counts per second. Below, we discuss the key capabilities and limitations of the most promising systems.

Colour centres in crystals

A wide range of crystal colour centres — fluorescent point defects — exist at low enough density that SPEs can be isolated (Fig. 1a). Many of these emitters are stable even at room temperature if the electronic ground and excited states are far from the host crystal's valence and conduction bands. Among the most thoroughly studied SPEs are colour centres in diamond[28]. Stable room-temperature operation is one of the biggest advantages of these systems as it enables rapid characterization and thus fast research and development cycles used to improve the material. The nitrogen–vacancy (NV) and the silicon–vacancy (SiV) defects in diamond are the most studied, and their crystallographic and electronic structures are established[28]. These centres can occur naturally in diamond and can also be produced by ion implantation and subsequent annealing. At low temperature (<5 K), the zero-phonon emission lines of both emitters are narrow enough to allow two-photon interference between different emitters, although the visibility is poor[29,30] (72 ± 5% and 66 ± 10% for the SiV and the NV centres, respectively).

The NV centre has a non-zero electronic dipole moment that causes its optical frequencies to be sensitive to local strain and electric fields, which in turn contributes to homogeneous and inhomogeneous broadening. These can be mitigated by growing better diamond host material or engineering dynamical schemes to control and offset the fluctuations[31]. On the other hand, defects with an inversion symmetry such as the SiV centre in diamond are less susceptible to local environmental fluctuations. Indeed, multiple nearly identical SiV centres can be grown in the same crystal, as was

Table 1 | Summary of photophysical properties of solid-state SPEs.

	Maximum count rate (without a cavity, continuous wave) (counts s^{-1})	Lifetime (ns)	Homogeneous linewidth at 4 K	Indistinguishable photons (IP) and entanglement (E)	Spatial targeted fabrication of single emitters	Operation temperature	Integration of SPEs with dielectric cavities or plasmonic resonators
Colour centres in diamond	SiV: ~3×10^6 (ref. 138)* NV: ~1×10^6 (ref. 139)† For other sources see ref. 28	SiV: ~1 NV: ~12–22	NV, SiV lifetime-limited[29,30] Cr-related: 4 GHz (ref. 140)	NV: IP, E SiV: IP	Only for NV and SiV (ref. 28)	RT	Dielectric: NV, SiV only Plasmonics: NV only
Defects in SiC, ZnO and BN Rare earths in YAG/YOS	YAG: ~60×10^3 (ref. 141) ZnO: ~1×10^5 (ref. 44) SiC: ~2×10^6 (ref. 35) BN: ~3×10^6 (ref. 56)	19 (ref. 49)§ 1–4 (ref. 44) 1–4 (ref. 35) ~3 (ref. 56)	N/A	No	No	RT	No
Arsenide QDs	~1×10^7 (ref. 84)‡	~1 (refs 6,84)	Lifetime-limited	Yes	Yes	4 K	Yes
Nitride QDs	N/A	~0.3 (ref. 85)	~1.5 meV (ref. 85)	No	Yes	RT	Dielectric: yes Plasmonics: no
CNTs	~3×10^3 (ref. 68)	~0.4 (ref. 68)	N/A	No	No	RT	Dielectric: yes Plasmonics: no
2D TMDCs	~3.7×10^5 (ref. 57)	~1–3 (ref. 57)	N/A	No	No	4 K	No

The reported count rates for each system can be potentially optimized by integrating with cavities or improving collection optics. *Reported from a nanodiamond on iridium. †Recorded from a nanodiamond positioned on a solid immersion lens. Similar values obtained by etching a bullseye grating into a diamond membrane[142]. In both cases emitters in bulk diamond are dimmer. ‡Count rate at the objective, which is directly comparable to other systems. §Realized by optical upconversion to a short-lived excited state. N/A, not available; RT, room temperature.

recently demonstrated[29,32]. The SiV centre also has a strong zero-phonon line (ZPL), with ~70% of photons emitted into the ZPL. Emission into the ZPL is important for photon-mediated entanglement of internal quantum states of multiple emitters. The brightness of the SiV centre in bulk diamond is, however, still low, owing to low quantum efficiency of the defect[28]. Other defects with similar symmetry and optical properties, for example germanium–vacancy centres[33,34], are currently being investigated as promising alternatives.

An important challenge for other documented diamond colour centres is to reveal unambiguously the precise crystallographic structure, symmetry and charge state of each emitter. Several defects with known crystallographic structures, such as the nickel-related NE8 centre (ZPL ~793 nm) and the nitrogen-related H3 defect (ZPL ~503 nm), have been isolated at the single-defect level, but controlled fabrication of these defects as single sites is still missing[28]. Studies into the NV centre provide an excellent toolkit and a clear pathway to do so. These studies should include atomistic modelling to elucidate the level structure of the other atom-like defects in solids. These studies may also assist in identifying other NV-like systems with efficient optical spin readout at room temperature in diamond and other wide-bandgap crystal hosts. Subsequently, engineering these defects could be attempted in a controlled manner.

Much recent work has also focused on colour centres in the compound semiconductors. Silicon carbide (SiC) is of particular interest, as its many polytypes also have a large bandgap (typically 3–4 eV) and its nuclear spins can be spin-free (that is, a nuclear spin state of zero), allowing for colour-centre spin states with long coherence times. Of practical importance is that SiC is grown on an industrial scale for semiconductor applications. Consequently, the discovery[35] of a bright room-temperature SPE in SiC, tentatively attributed to the positively charged carbon antisite-vacancy (C_vC_{Si}) defect[36], was shortly followed by the first report of a pulsed room-temperature SPE diode[37]. Detection and manipulation of the spin state of SPEs in SiC has, however, been demonstrated so far only in comparatively low-brightness emitters attributed to Si vacancy and di-vacancy defects[38–42]. A conclusive correlation between the emission properties, spin properties and the precise crystallographic structure of each defect is yet to be established, and a topic of active research pursued by numerous groups[43].

The wide-bandgap (3.4 eV at room temperature) II–VI compound semiconductor ZnO has optoelectronic properties that could offer additional degrees of control over incorporated SPEs, including piezoelectric and spintronic properties, as well as mature commercial growth and processing. Several types of SPE have been reported in ZnO, but the structural origin of these luminescent centres is controversial, and most of the emitters reported so far suffer from blinking and bleaching[44–48]. Moreover, fabrication of high-quality, stable p-doped ZnO has remained elusive despite intense research efforts. This problem must be solved to enable the fabrication of ZnO p–n junctions and associated devices, a key potential benefit of this SPE host.

By comparison, rare-earth-ion impurities in crystals such as yttrium aluminium garnet (YAG) and yttrium orthosilicate (YOS) are well characterized and understood, with a range of properties that make them compelling candidates for SPEs[49–53]. These include narrow optical emission lines arising from transitions between excited states that are efficiently screened by outer-lying shells from the enclosing environment and hyperfine split ground states with very long coherence times[54,55]. Many of the garnet host materials have well-established growth protocols, driven by industrial applications such as solid-state laser gain materials. However, the excited-state lifetimes tend to be long, sometimes hundreds of milliseconds or more, resulting in low photon emission rates that make the detection of single ions challenging, and limit the maximum count rate of a practical SPE. This limitation has been partly circumvented in the case of Pr:YAG using a two-step upconversion process that has the mutual benefit of accessing a short-lived excited state and avoiding high background levels[49]. Nonetheless, maximum reported count rates are still moderate (~60×10^3; see Table 1) owing in part to a multitude of competing relaxation pathways.

The natural linewidths of all the colour centres need to be investigated in more detail. Although several lifetime-limited linewidths have been demonstrated in diamond, the existence of such linewidths has not been demonstrated for colour centres in other systems. Given the complexity of dielectric environments typically encountered in the proximity of defects, it is important to continue developing emitter systems that are inherently more tolerant to

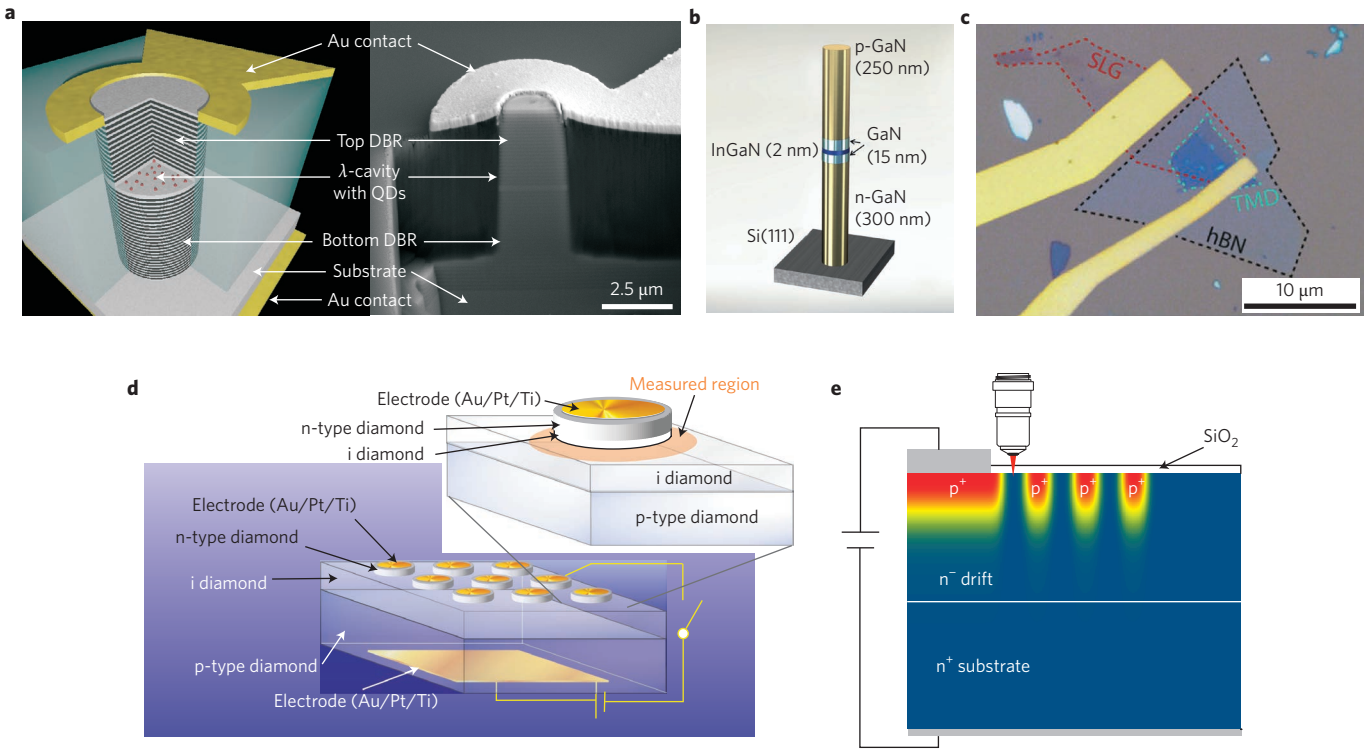

Figure 2 | Electrically driven single-photon emitters. a, InAs QDs embedded in an AlAs/GaAs Bragg-stack micropillar cavity that is doped to form a p–n structure used to electrically excite the QDs. DBR, distributed Bragg reflector. **b**, An InGaN QD embedded in a p–n nanowire made of p-GaN and n-GaN, grown on a silicon substrate. **c**, First demonstration of a quantum light-emitting device made using a 2D material. The TMDC is sandwiched between hBN and single-layer graphene (SLG). **d**, Diamond quantum LED realized by exciting the neutral NV centres in a diamond p–i–n structure. **e**, SiC-based quantum LED realized by creating a p^+–n^- junction and exciting emitters at the interface. Figure reproduced with permission from: **a**, ref. 94, AIP Publishing LLC; **b**, ref. 95, Nature Publishing Group; **c**, ref. 96, Nature Publishing Group; **d**, ref. 98, Nature Publishing Group; **e**, ref. 37, Nature Publishing Group.

stray electric fields, as well as active emitter stabilization methods to stabilize spectral drift[31].

Two-dimensional materials

Recently, a number of 2D materials have been shown to host SPEs[56–63] (Fig. 1b). The 2D hosts include transition metal dichalcogenides (TMDCs) in which the quantum defects are ascribed to localized, weakly bound excitons, and hexagonal boron nitride (hBN) in which SPEs have been associated with defects deep within the bandgap. Similarly to QDs, the TMDCs only exhibit quantum emission at cryogenic temperatures, whereas defects in hBN give rise to deep states that allow SPE operation at room temperature. The nature of SPEs in TMDCs is yet to be clarified. The emission is detuned by several millielectronvolts from the exciton transition and often appears at the 2D flake edges. The brightness varies from sample to sample, and most of the lines exhibit strong Zeeman shifts with applied magnetic field that could potentially be used to tune multiple emitters to the same frequency and realize photon indistinguishability. Several groups are pursuing this avenue of research[57–63].

Further research is required to explore limits of linewidth (for example through resonant excitation), photon purity and internal quantum efficiency of SPEs in 2D materials. Nevertheless, 2D materials offer a fascinating platform for quantum photonics. Given that the SPEs are embedded in a monolayer, total internal reflection can be avoided (which is a big problem with colour centres), and the light extraction efficiency can be very high. Moreover, integration with cavities and photonic waveguides is promising since manipulation of 2D materials on various substrates is now established. Another advantage of the defects in 2D materials is the great potential for coupling them to plasmonic structures. The thickness of the host material is particularly important for coupling to plasmonic tips or plasmonic gap cavities, as these require nanometre-scale proximity that is typically difficult for SPEs in bulk emitters in bulk crystals.

Defects in hBN are the most recent addition to the SPE library[64–67] and among the brightest SPEs reported so far[56]. Megahertz count rates at the detector have been recorded[56] with a very low excitation power of several hundred microwatts. The majority of photons are emitted into the ZPL, although the ZPL wavelength can vary from sample to sample. Rigorous modelling along with resonant excitation need to be carried out to reveal the electronic and crystallographic structure of the emitters. The natural linewidths of these emitters seem to be broadened by spectral diffusion, but these deficiencies may be resolved using dynamic stabilization[31].

Carbon nanotubes

Semiconducting CNTs (Fig. 1c) have also been shown to host SPEs[68–70]. The biggest promise for CNTs is the potential realization of optomechanical circuits since the CNT is a high-quality 1D mechanical resonator. Its mechanical properties are mostly known, and the growth of long CNTs is established. Another unique aspect of CNT SPEs is that the ZPLs can be above 1 μm in wavelength, potentially lowering the barrier for integration with existing telecom technologies.

The origin of these emitters is ascribed to excitons bound by shallow QD-like states generated by environmental fluctuations. These emitters therefore operate only at cryogenic temperatures and are highly susceptible to blinking, bleaching and dephasing. Recently, room-temperature quantum emission has been observed from deep O-related impurity states[68]. These emitters, however, require further characterization, and an outstanding challenge with all CNT emitters is to increase the brightness and stability of the SPEs.

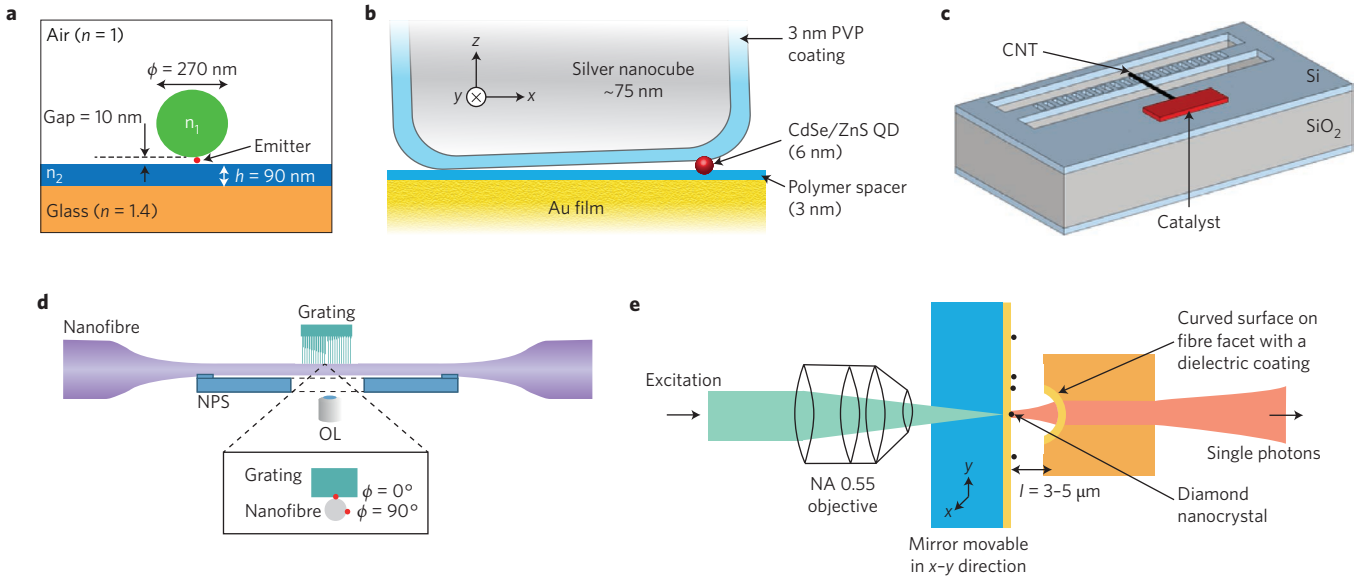

Figure 3 | Coupling single emitters to optical resonators. a, A single emitter (CdSe/ZnS QD) placed inside a dielectric slot cavity. The cavity is formed by positioning a silicon nanowire (n_1, green) on a ZnS slab (n_2, blue). The geometry enables a Purcell enhancement of up to 31. **b**, A CdSe/ZnS QD is placed in a nanogap spacer between a silver cube and a gold film. This geometry results in a 1,900-fold increase in emission rate. PVP, poly(vinyl pyrrolidone). **c**, A CNT hosting individual emitters positioned on top of a nanobeam cavity, resulting in a 10-fold enhancement of luminescence. **d**, A single QD is positioned in a grating, mounted on top of a nanofibre. This geometry enables coupling of the enhanced emission directly into the fibre-guided mode. OL, objective lens; NPS, nanopositioning stage. **e**, Nanodiamonds with single NV centres coupled to a fibre-based microcavity. This geometry can enable up to 65% of the NV emission to be channelled into the cavity mode. *l*, cavity length; NA, numerical aperture. Figure reproduced with permission from: **a**, ref. 107, American Chemical Society; **b**, ref. 108, American Chemical Society; **c**, ref. 109, Nature Publishing Group; **d**, ref. 110, APS; **e**, ref. 111, APS.

Other 1D hosts include QD-containing nanowires. A particularly interesting case is that of crystal-phase QDs, formed by modifying the crystallographic structure (from zinc blende to wurtzite) but not the chemical composition during the nanowire growth[71]. The quantum confinement originates from the bandgap differences at the domain interfaces within the nanowire.

Quantum dots

Self-assembled InAs/GaAs QDs (Fig. 1e) currently have the highest all-around SPE performance[72–75]. Emitted photons have been entangled to the spin degree of an additional electron loaded on the QD[4], and two-photon entangled states have been produced using bi-exciton cascade[76,77]. Under resonant excitation, recent demonstrations have achieved photon purity >99% (that is, $g^{(2)}(0) < 0.01$), and photon collection efficiency in excess of 75%[24,25,76–79]. In a recent report, over 1,000 consecutive emitted photons exhibited more than 92% indistinguishability[27]. A variety of methods have been developed to increase photon extraction efficiency above 50%, including coupling QDs to micropillars, nanowire antennas[80–82], microlenses[83] or circular Bragg grating bullseye cavities[84] defined on top of a pre-characterized dot. Moreover, strong coupling of single dots to photonic crystal cavities has been thoroughly investigated, bringing this platform one step closer towards integrated photonics on a single chip and engineering of spin/photon interfaces[1,2].

The production of many-photon quantum states can, to some extent, be achieved by time-delaying emissions from a single QD, but at the loss of overall rate. To maintain a high rate of multiphoton state generation, a key challenge for the InAs QDs is reproducibility of the samples and growth of multiple identical dots. To better interface with telecom systems, there has also been noticeable progress towards infrared emitters, and two-photon interference was recently demonstrated from InAs/InP SPEs in the telecom spectrum (1,550 nm)[26].

There has also been considerable progress in III-nitride QDs that operate even at room temperature[85–87]. But owing to challenges in growth of high-quality material and a higher emission energy of ~3 eV, their use as a reliable SPE platform with high signal-to noise ratio and a relatively low $g^{(2)}(0)$ is yet to be demonstrated.

Finally, perovskite QDs (not included in Table 1) have been shown to exhibit quantum emission[88] and operate at room temperature. However, the emitters blink and bleach, and the reported count rates are low. More materials development is required to optimize these emitters.

Electrically driven devices

Deployment of scalable single-photon technologies can benefit from electrically triggered devices integrated onto a single chip[89–93]. Figure 2 shows electrically driven quantum LEDs (QLEDs) that have been realized with QDs (Fig. 2a,b)[94,95], 2D TMDCs[96,97] (Fig. 2c) and defects in solids (Fig. 2d,e)[37,98,99]. One of the main challenges in QLEDs is to concentrate the electron–hole pair recombination current on the defect or QD of interest rather than on surrounding impurities. Therefore, material growth and site-specific emitter engineering are key to achieving working devices and technologies that are efficient and scalable. Indeed, generation of efficient QLEDs has been realized in the GaAs system[100], which allows for p- and n-type doping as well as positioning of QDs. Moreover, the QLEDs have been combined with photonic structures such as Bragg reflectors or nanowires that further enhance the overall efficiency of the devices (Fig. 2a,b). Entanglement between emitted photon pairs has also been recently reported — a hallmark of scalable quantum technologies[78].

In wide-bandgap systems, including diamond and silicon carbide, charge injection has so far resulted in increased background emission due to high defect concentration, and therefore reduced signal-to-noise ratio of the sources. A unique challenge for electrical driving concerns the control of the charge state, which greatly changes the emission spectrum in colour centres (whereas the shift between excitons and trions in QDs is typically smaller). While the negatively charged NV centre is of interest to the quantum photonic

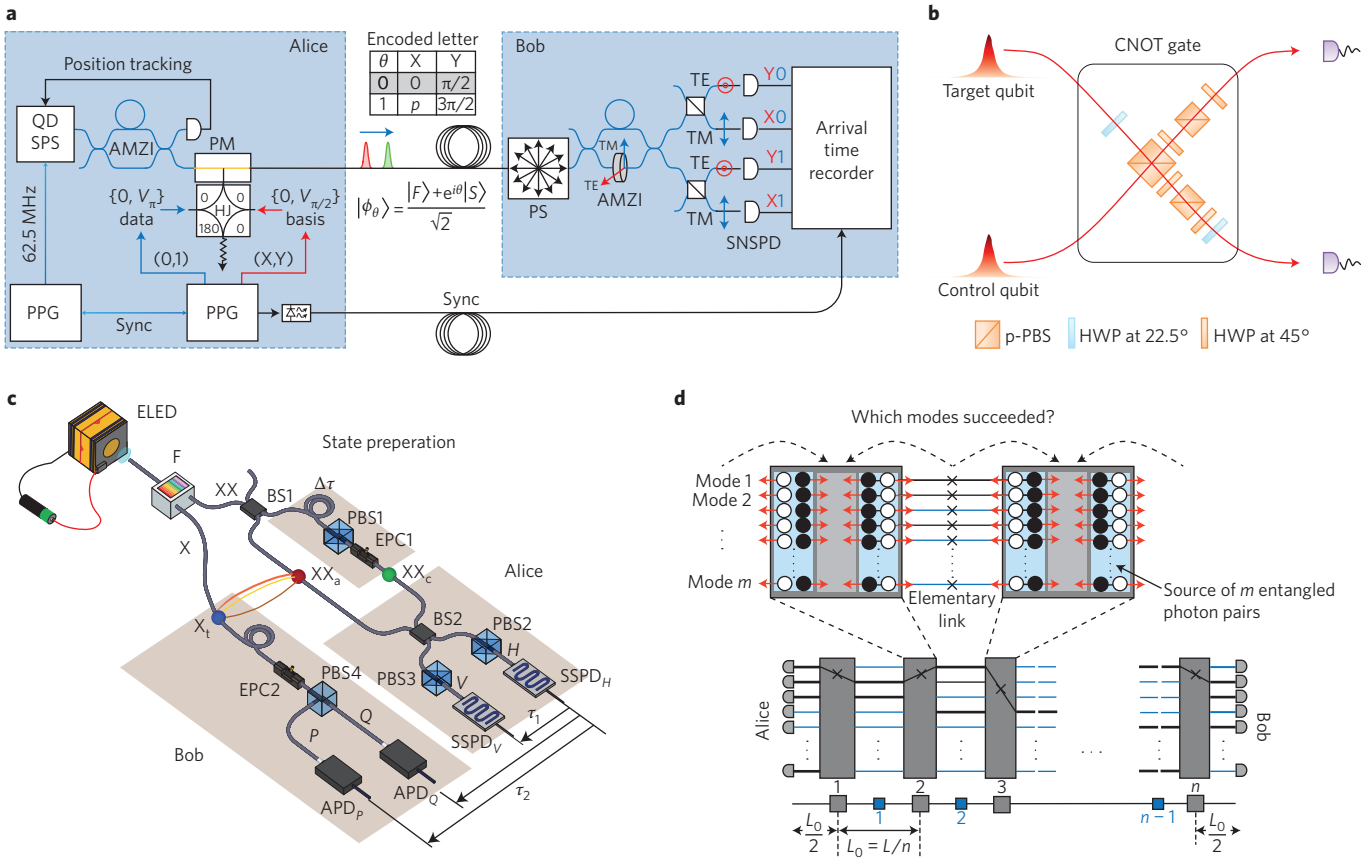

Figure 4 | Applications of quantum emitters. a, Quantum key distribution protocol realized over 120 km using an InAs/InP QD and a superconductor detector. AMZI, asymmetric Mach–Zehnder interferometer; HJ, hybrid junction; PPG, pulse pattern generator; PS, polarization scrambler; SPS, single-photon source; SNSPD, superconducting nanowire single-photon detector; TE, transverse electric; TM, transverse magnetic. **b**, A post-selected optical CNOT gate implemented using a nearly 'perfect' InAs QD. HWP, half-wave plate; PBS, polarizing beam-splitter. **c**, A quantum teleportation scheme realized with an electrically driven QD. APD, avalanche photodiode; BS, beam splitter; ELED, entangled-light-emitting diode; EPC, electrical polarization controller; F, spectral filter; SSPD, superconducting single-photon counting detector; *P*, *Q*, *V* and *H* are photons labelled by their polarization; τ, time delay. **d**, Schematic illustration of a quantum repeater. Chain of elementary links for a repeater architecture that uses quantum memories, Bell-pair sources, probabilistic Bell-state measurement, and multiplexing over *m* orthogonal qubit modes (parallel channels). Grey (blue) are major (minor) nodes. Figure reproduced with permission from: **a**, ref. 115, under a Creative Commons licence (http://creativecommons.org/licenses/by/4.0/); **b**, ref. 122, Nature Publishing Group; **c**, ref. 123, Nature Publishing Group; **d**, ref. 118, M. Pant *et al*.

community, only the neutral NV centre can be driven electrically. Electrical pumping of other colour centres — such as diamond Xe centres[101] or SiV centres[102] — appears promising.

Finally, 2D TMDCs provide another promising platform for QLED systems, as p–n junctions can now be fabricated in a wide range of homo- and heterojunctions, sheet conductivity can be high, and current could be injected with extremely high spatial resolution, at least in the out-of-plane dimension. In addition, charge control of individual shallow defects in hBN/graphene heterostructures using a high-resolution scanning tunnelling microscope has recently been shown[103]. This result opens interesting perspectives towards voltage-controlled emission from SPEs in hBN.

Integrated systems

In many applications, it is beneficial to integrate SPEs on-chip with other photonic devices, including photonic cavities, filters, waveguides, resonators and detectors. The integrated systems enable light guidance on a chip, enhancement of emission rates by modification of spontaneous emission, and efficient photonic interfaces to atom-like emitters in the strong Purcell and strong-coupling regimes[1,2,6,104]. Two broad approaches have been investigated to integrate quantum emitters and photonic integrated circuits (PICs): either a hybrid approach[105,106] whereby the SPE is heterogeneously integrated with a PIC made of a different material, or a homogeneous approach in which the SPE is monolithically grown in the PIC device[1,73]. Each approach offers advantages and disadvantages. In the following, we focus only on the hybrid approach as it offers more flexibility for realizing the final device. We note that colloidal QDs have been used in much of the proof-of-concept work done so far because they are relatively easy to fabricate and manipulate. Experiments to date have found unstable optical emission, however, and therefore we do not include them among the most promising SPEs in this Review.

Figure 3 summarizes several key experiments on hybrid integration of SPEs into cavities and waveguides. Figure 3a and b shows single colloidal CdSe/ZnS QDs coupled to a dielectric slot waveguide and a plasmonic gap cavity, respectively[107,108]. The latter results in a large emission rate enhancement of up to ~1,900 (ref. 108). Figure 3c shows a CNT that hosts a quantum emitter coupled to a nanobeam cavity in a low mode volume silicon photonic crystal that results in an emission enhancement, and a theoretical Purcell value of ~300 (ref. 109). Figure 3d and e shows examples of fibre-based cavities, realized with QDs[110] and nanodiamonds[111], respectively. Although such architectures are not easy to fabricate, they offer an interesting advantage in that the emission is directed into an optical fibre and can be easily integrated with other photonic components.

Table 2 | Summary of source requirements for different applications.

	Photon purity $g^{(2)}(0)$	Indistinguishability	Efficiency η	Repetition rate
Quantum key distribution	<0.1	Not critical, but consecutive photons must be uncorrelated	>0.5*	>GHz
Cluster-state quantum computing	<0.001 (more study needed on many-photon errors)	>0.99	>0.99 for reasonable resources	Ideally GHz to avoid long buffers, maximize experiment frequency
All-optical quantum repeater	<0.001	>0.99	>0.99	>GHz
Bell-state sources for memory-based repeaters	<0.01	>0.9	>0.9	Ideally GHz

*To be competitive against attenuated laser quantum key distribution with decoy state.

While the results presented in Fig. 3 are promising, there are several difficulties in assembling these hybrid nanophotonic systems. (1) The dipole orientation of the SPE within the solid-state particle is unknown, and once manipulated into a cavity, it is unlikely to experience the strongest electromagnetic field. (2) The SPEs are never located precisely in the 'middle' of the foreign particle, which poses limitations on the cavity design. (3) The actual placement of the particle in the strongest cavity field is often challenging. (4) The particles containing the SPEs scatter light, which degrades the cavity resonances and adds loss channels. The recently discovered SPEs in 2D materials may solve these problems, as the optical dipole is typically in-plane, aiding angular alignment, and the atomic thinness of the host material causes only minimal perturbations to the waveguide or cavity mode. Indeed, initial experiments on coupling exciton transitions of 2D materials to optical cavities are encouraging[112]. With improved control over lateral engineering of SPEs in these materials, high-precision deterministic coupling to cavities should become achievable.

Applications of SPEs

System-level demands on quantum light sources are far more stringent than for their classical counterparts, as reflected for example in the extremely high internal and extraction efficiency requirements in Table 2. For instance, most quantum key distribution (QKD) systems are nowadays run with attenuated laser sources, and can operate with a mean photon number per pulse of $\langle n \rangle \approx 0.5$ (using recently introduced decoy-state protocols[113,114] to counter the photon-number splitting side-channel attack). An ideal SPE could push this to $\langle n \rangle = 1$. Thus, to make SPEs worthwhile on the sender side (Alice), the efficiency from the source to the fibre, including all state preparation (for example polarization encoding), should be at least 0.5. Recent results demonstrated QKD with triggered SPEs over more than 120 km in fibres (Fig. 4a)[115]. The raw and secure key rates at 100 km were ~80 and 28 bits per second, respectively, realized with true pure SPEs ($g^{(2)}(0) \approx 10^{-3}$). But this rate is still 1–2 orders of magnitude slower than attenuated-laser QKD, pointing to the need for improvements in the source brightness and extraction efficiencies for SPEs to become competitive for QKD[113,115].

While QKD does not need — but could benefit from — SPEs, other applications require them. One important area is in the production of many-photon entangled states. For instance, heralded two-photon Bell states can be produced using linear optics and four single photons. Heralded Bell states are useful for certain types of quantum repeater protocols using atomic memories[116]. SPEs are also central resources for producing cluster states for all-optical quantum repeaters[117], although the latter is likely to require photon source efficiencies over 0.99 to keep the number of required sources manageable[118]. Fault-tolerant quantum computing imposes similar efficiency requirements on the source[88,119], as well as near-unity indistinguishability and probably very high photon purity, although the effect of multiphoton emissions on gate fidelities has not yet been thoroughly analysed[8]. Encouragingly, theoretical work on percolation-based generation of photonic cluster states shows significant loss tolerance. Even the best theoretical protocols, however, call for at least thousands of photons per encoded quantum bit, so many identical sources will need to work together efficiently, probably on PICs. A more forgiving application could be boson sampling and photonic quantum walks[9,120], which promise to beat today's classical computers at specialized tasks with more than ~40 photons; these applications can also tolerate lower indistinguishability[121].

Two-qubit logic gates and quantum-state teleportation (Fig. 4b,c)[122,123] represent operational primitives of photonic quantum information processing. A post-selected optical quantum-controlled NOT (CNOT) gate (analogous to a logic NOT gate) was recently demonstrated with indistinguishable SPEs (Fig. 4b). A heralded CNOT gate together with feed-forward and single-qubit rotation produces a universal set gate for quantum computing[7,117,118]. Finally, Fig. 4d illustrates the recently proposed concept of an all-optical quantum repeater for long-haul quantum cryptographic links. Quantum repeaters are analogous to amplifiers in classical channels[117]. They are proposed to be inserted between distant quantum nodes to generate a shared secret key to compensate for the losses in the channel[118]. Based on recent resource-cost analysis[118], millions of high-performance SPEs would be needed per repeater node to produce the required cluster states needed to beat the limits of repeaterless QKD. Additional theoretical work is needed to elucidate requirements on photon purity and indistinguishability, although errors in both will probably need to be much below 1%.

The early discovery of QD SPEs and their continued refinement has allowed these systems to lead the way in key quantum optics demonstrations, including CNOT gates and spin-photon entanglement experiments. However, the applications of atom-like defects in solids have grown in recent years far beyond single-photon emission. For example, defects in wide-bandgap systems (such as NV centres in diamond) have emerged as excellent systems for nanoscale sensing[124] and long-range electron-spin entanglement[125], while rare-earth-ion systems are being engineered as promising quantum memories for quantum repeaters.

Conclusions and outlook

SPEs have been, and remain, of central importance in many quantum optics applications. The basic physics of two-level optical systems is well established, but coaxing solid-state emitter systems, with their often complex mesoscopic environment, to simply fit such simple models has not been possible. Instead, the challenges of developing 'ideal' single-photon sources have prompted successful research that has greatly elucidated physical processes in open quantum systems and advanced our understanding on quantum–classical boundaries. These research efforts have also led to pleasant surprises — for instance, that the apparent 'nuisance' of emitter electron spins coupling to nearby nuclei actually allows controllable access of ancilla nuclear spins and related research activities.

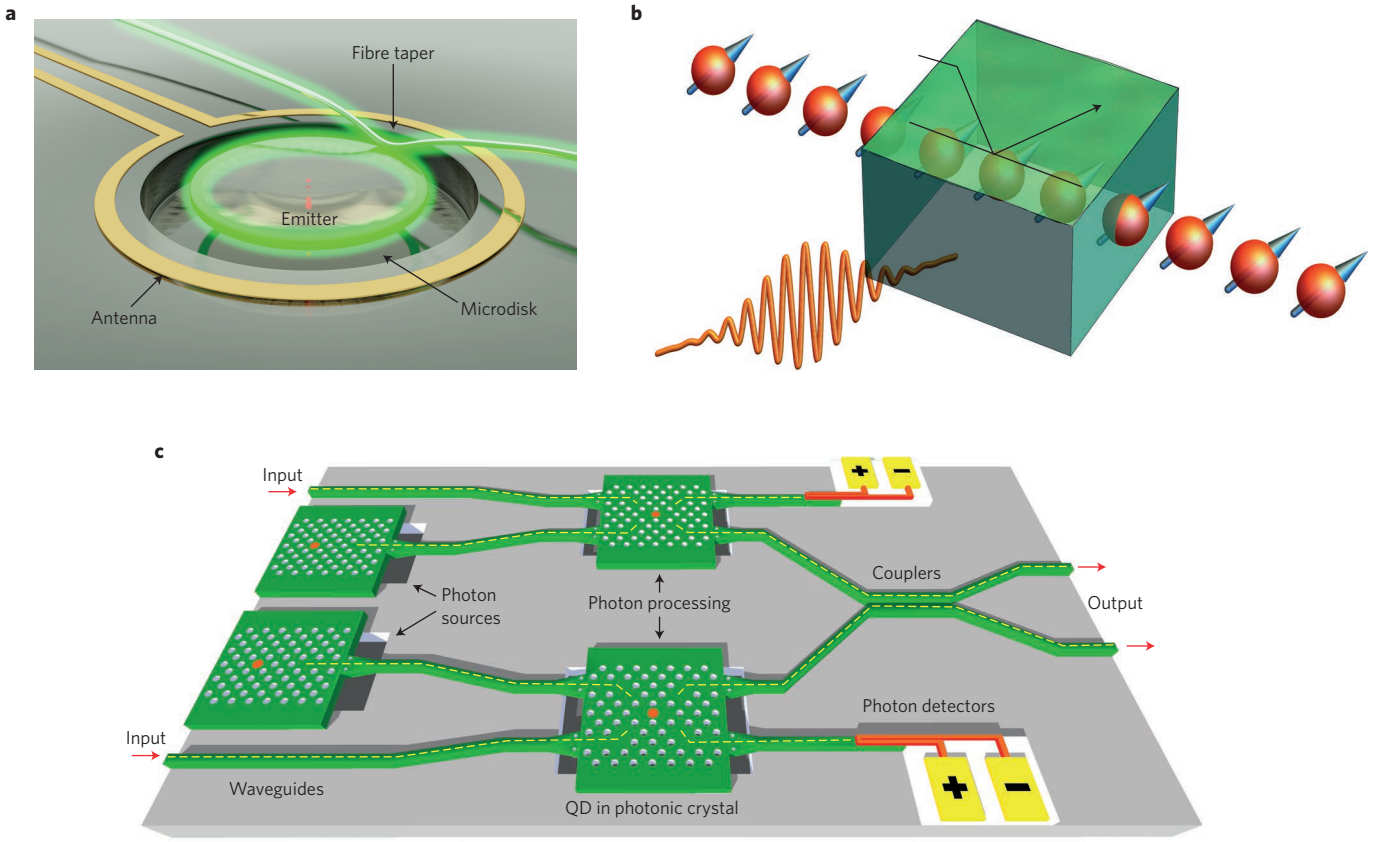

Figure 5 | Future applications of solid-state single emitters. a, Optomechanics with single photons. Coupling between single photons and single mechanical oscillations. Experiments of this type are already under way. **b**, Schematic illustration of a single-photon transistor. Such a device has been proposed and realized using Rydberg states in an ultracold Rb gas as well as single molecules. An analogous device is yet to be demonstrated using solid-state defect-based emitters. **c**, On-chip integrated quantum memory and quantum circuitry. Although such a memory has been realized with atomic vapour, and individual quantum memories have been demonstrated with both NV centres and QDs, on-chip integration is yet to be achieved. Figure courtesy of D. Lake and P. Barclay, Univ. of Calgary (**a**); R. Johne and A. Fiore, Eindhoven Univ. Technology (**c**).

Rapid progress in a range of SPE technologies has greatly improved key metrics — photon purity, efficiency and indistinguishability — as well as important practical matters including reproducibility, wavelength and electrical pumping. SPEs are now close to improving on state-of-the-art technologies, including photon-number-squeezed light sources for intensity standards or boson sampling and related applications. With sufficient overall internal and external photon efficiency, single-photon sources stand to become competitive for quantum communications — as sources for QKD and for augmenting quantum repeaters based on matter-based long-lived memories. Finally, when the key performance metrics of efficiency, indistinguishability and purity have errors below 1% or so, one may expect SPEs to enable scalable production of many-photon entangled states for advanced applications including all-optical repeaters and quantum repeating in linear optics.

Reaching the performance requirements for these applications requires continued basic research as well as engineering of already established systems. The crystallographic and electronic level structure of most of the current defects is still under debate. Rigorous atomistic modelling along with established spectroscopic, electron spin resonance and ion implantation studies is needed. The tremendous improvements in growth of arsenide-based systems can be extended to the increasingly important optoelectronic material system of III-nitrides, with a particular focus on reducing inhomogeneous broadening through improved material growth and methods for control of individual SPEs, particularly in attempts to grow identical QDs. After the discovery of a whole new class of SPEs in 2D materials with unique optical and material properties, experimental and theoretical work are needed to elucidate the photophysics, crystallographic and electronic properties, and methods of production. Growth of alternating layers promises multicolour SPEs on a chip, and recent progress in 2D-material electrical contacts promises high-performance electrically driven SPE devices. Thorough optical studies are needed, however, to understand the possible limits to efficiency, indistinguishability and photon purity. Ultimately, whereas miniaturization of electronic devices will reach the level of single charges, miniaturization of photonic and optoelectronic components will require manipulation of SPEs in a microscopic solid-state environment.

Among other promising applications in which SPEs can play a central role is quantum optomechanics, which may revolutionize today's sensing technologies[126]. Cooling an optomechanical resonator to its ground state has been demonstrated, and interfacing mechanical motion with spins and single photons is an exciting new direction of research. One promising avenue is to explore strain to mediate coupling between optical and mechanical resonances in a monolithic integrated device[127–129]. The mature nanofabrication capabilities of diamond or silicon carbide are promising for such devices (Fig. 5a)[130–133].

Another promising direction includes single-photon-level 'transistors' (Fig. 5b). Such advances will enable explorations of quantum nonlinearities and open the path for discoveries of new physical phenomena. Indeed, a single-photon transistor has been realized with trapped rubidium atoms[134] and single molecules[135], but is yet

to be realized in the solid state[136,137]. Finally, many proposals for cluster-state production would benefit greatly from an electrically triggered source of entangled photons that are guided and stored on a single chip (Fig. 5c). The required toolkit is in place, primarily because a vast library of SPEs has already been established. It is therefore the right time to dedicate resources to scalability, optimization and applicability of these emitters to real devices.

Received 29 June 2016; accepted 18 August 2016;
published online 29 September 2016

References

1. O'Brien, J. L., Furusawa, A. & Vuckovic, J. Photonic quantum technologies. *Nat. Photon.* **3,** 687–695 (2009).
2. Lodahl, P., Mahmoodian, S. & Stobbe, S. Interfacing single photons and single quantum dots with photonic nanostructures. *Rev. Mod. Phys.* **87,** 347–400 (2015).
3. Koenderink, A. F., Alù, A. & Polman, A. Nanophotonics: shrinking light-based technology. *Science* **348,** 516–521 (2015).
4. Gao, W. B., Imamoglu, A., Bernien, H. & Hanson, R. Coherent manipulation, measurement and entanglement of individual solid-state spins using optical fields. *Nat. Photon.* **9,** 363–373 (2015).
5. Northup, T. E. & Blatt, R. Quantum information transfer using photons. *Nat. Photon.* **8,** 356–363 (2014).
6. Buckley, S., Rivoire, K. & Vuckovic, J. Engineered quantum dot single-photon sources. *Rep. Prog. Phys.* **75,** 126503 (2012).
7. Kok, P. *et al.* Linear optical quantum computing with photonic qubits. *Rev. Mod. Phys.* **79,** 135–174 (2007).
8. Gimeno-Segovia, M., Shadbolt, P., Browne, D. E. & Rudolph, T. From three-photon Greenberger–Horne–Zeilinger states to ballistic universal quantum computation. *Phys. Rev. Lett.* **115,** 020502 (2015).
9. Aspuru-Guzik, A. & Walther, P. Photonic quantum simulators. *Nat. Phys.* **8,** 285–291 (2012).
10. Aharonov, D., Ambainis, A., Kempe, J. & Vazirani, U. in *Proc. 33rd Annual ACM Symposium on Theory of Computing* 50–59 (ACM, 2001).
11. Aaronson, N. N. P. & Arkhipov, A. in *Proc. 43rd Annual ACM Symposium on Theory of Computing* 333–342 (ACM, 2011).
12. Giovannetti, V., Lloyd, S. & Maccone, L. Advances in quantum metrology. *Nat. Photon.* **5,** 222–229 (2011).
13. Scarani, V. *et al.* The security of practical quantum key distribution. *Rev. Mod. Phys.* **81,** 1301–1350 (2009).
14. Lo, H.-K., Curty, M. & Tamaki, K. Secure quantum key distribution. *Nat. Photon.* **8,** 595–604 (2014).
15. Cheung, J. Y. *et al.* The quantum candela: a re-definition of the standard units for optical radiation. *J. Mod. Opt.* **54,** 373–396 (2007).
16. Chu, X.-L., Götzinger, S. & Sandoghdar, V. A high-fidelity photon gun: intensity-squeezed light from a single molecule. Preprint at https://arXiv.org/abs/1608.07980 (2016).
17. Kimble, H. J., Dagenais, M. & Mandel, L. Photon antibunching in resonance fluorescence. *Phys. Rev. Lett.* **39,** 691–695 (1977).
18. Kuhn, A., Hennrich, M. & Rempe, G. Deterministic single-photon source for distributed quantum networking. *Phys. Rev. Lett.* **89,** 067901 (2002).
19. Howell, J. C., Bennink, R. S., Bentley, S. J. & Boyd, R. W. Realization of the Einstein–Podolsky–Rosen paradox using momentum- and position-entangled photons from spontaneous parametric down conversion. *Phys. Rev. Lett.* **92,** 210403 (2004).
20. Kwiat, P. G. *et al.* New high-intensity source of polarization-entangled photon pairs. *Phys. Rev. Lett.* **75,** 4337–4341 (1995).
21. Yan, Z. *et al.* Generation of heralded single photons beyond 1100 nm by spontaneous four-wave mixing in a side-stressed femtosecond laser-written waveguide. *Appl. Phys. Lett.* **107,** 231106 (2015).
22. Koehl, W. F., Seo, H., Galli, G. & Awschalom, D. D. Designing defect spins for wafer-scale quantum technologies. *MRS Bull.* **40,** 1146–1153 (2015).
23. Loredo, J. C. *et al.* Scalable performance in solid-state single-photon sources. *Optica* **3,** 433–440 (2016).
24. Somaschi, N. *et al.* Near-optimal single-photon sources in the solid state. *Nat. Photon.* **10,** 340–345 (2016).
25. Ding, X. *et al.* On-demand single photons with high extraction efficiency and near-unity indistinguishability from a resonantly driven quantum dot in a micropillar. *Phys. Rev. Lett.* **116,** 020401 (2016).
26. Kim, J.-H., Cai, T., Richardson, C. J. K., Leavitt, R. P. & Waks, E. Two-photon interference from a bright single-photon source at telecom wavelengths. *Optica* **3,** 577–584 (2016).
27. Wang, H. *et al.* Near-transform-limited single photons from an efficient solid-state quantum emitter. *Phys. Rev. Lett.* **116,** 213601 (2016).
28. Aharonovich, I. & Neu, E. Diamond nanophotonics. *Adv. Opt. Mater.* **2,** 911–928 (2014).
29. Sipahigil, A. *et al.* Indistinguishable photons from separated silicon-vacancy centers in diamond. *Phys. Rev. Lett.* **113,** 113602 (2014).
30. Sipahigil, A. *et al.* Quantum interference of single photons from remote nitrogen-vacancy centers in diamond. *Phys. Rev. Lett.* **108,** 143601 (2012).
31. Acosta, V. M. *et al.* Dynamic stabilization of the optical resonances of single nitrogen-vacancy centers in diamond. *Phys. Rev. Lett.* **108,** 206401 (2012).
32. Rogers, L. J. *et al.* Multiple intrinsically identical single-photon emitters in the solid state. *Nat. Commun.* **5,** 4739 (2014).
33. Ralchenko, V. G. *et al.* Observation of the Ge-vacancy color center in microcrystalline diamond films. *Bull. Lebedev Phys. Inst.* **42,** 165–168 (2015).
34. Iwasaki, T. *et al.* Germanium-vacancy single color centers in diamond. *Sci. Rep.* **5,** 12882 (2015).
35. Castelletto, S. *et al.* A silicon carbide room-temperature single-photon source. *Nat. Mater.* **13,** 151–156 (2014).
36. Umeda, T. *et al.* Identification of the carbon antisite–vacancy pair in 4H-SiC. *Phys. Rev. Lett.* **96,** 145501 (2006).
37. Lohrmann, A. *et al.* Single-photon emitting diode in silicon carbide. *Nat. Commun.* **6,** 7783 (2015).
38. Koehl, W. F., Buckley, B. B., Heremans, F. J., Calusine, G. & Awschalom, D. D. Room temperature coherent control of defect spin qubits in silicon carbide. *Nature* **479,** 84–87 (2011).
39. Falk, A. L. *et al.* Polytype control of spin qubits in silicon carbide. *Nat. Commun.* **4,** 1819 (2013).
40. Riedel, D. *et al.* Resonant addressing and manipulation of silicon vacancy qubits in silicon carbide. *Phys. Rev. Lett.* **109,** 226402 (2012).
41. Christle, D. J. *et al.* Isolated electron spins in silicon carbide with millisecond coherence times. *Nat. Mater.* **14,** 160–163 (2015).
42. Widmann, M. *et al.* Coherent control of single spins in silicon carbide at room temperature. *Nat. Mater.* **14,** 164–168 (2015).
43. Lienhard, B. *et al.* Bright and stable visible-spectrum single photon emitter in silicon carbide. *Optica* **3,** 768–774 (2016).
44. Morfa, A. J. *et al.* Single-photon emission and quantum characterization of zinc oxide defects. *Nano Lett.* **12,** 949–954 (2012).
45. Neitzke, O. *et al.* Investigation of line width narrowing and spectral jumps of single stable defect centers in ZnO at cryogenic temperature. *Nano Lett.* **15,** 3024–3029 (2015).
46. Jungwirth, N. R. *et al.* A single-molecule approach to ZnO defect studies: single photons and single defects. *J. Appl. Phys.* **116,** 043509 (2014).
47. Jungwirth, N. R., Chang, H.-S., Jiang, M. & Fuchs, G. D. Polarization spectroscopy of defect-based single photon sources in ZnO. *ACS Nano* **10,** 1210–1215 (2016).
48. Choi, S. *et al.* Single photon emission from ZnO nanoparticles. *Appl. Phys. Lett.* **104**, 261101 (2014).
49. Kolesov, R. *et al.* Optical detection of a single rare-earth ion in a crystal. *Nat. Commun.* **3,** 1029 (2012).
50. Xia, K. *et al.* All-optical preparation of coherent dark states of a single rare earth ion spin in a crystal. *Phys. Rev. Lett.* **115,** 093602 (2015).
51. Emanuel, E., Tobias, U., Stephan, G. & Vahid, S. Spectroscopic detection of single Pr^{3+} ions on the $^3H_4$–$^1D_2$ transition. *New J. Phys.* **17,** 083018 (2015).
52. Utikal, T. *et al.* Spectroscopic detection and state preparation of a single praseodymium ion in a crystal. *Nat. Commun.* **5,** 3627 (2014).
53. Kolesov, R. *et al.* Mapping spin coherence of a single rare-earth ion in a crystal onto a single photon polarization state. *Phys. Rev. Lett.* **111,** 120502 (2013).
54. Zhong, T., Kindem, J. M., Miyazono, E. & Faraon, A. Nanophotonic coherent light-matter interfaces based on rare-earth-doped crystals. *Nat. Commun.* **6,** 8206 (2015).
55. Longdell, J. J., Fraval, E., Sellars, M. J. & Manson, N. B. Stopped light with storage times greater than one second using electromagnetically induced transparency in a solid. *Phys. Rev. Lett.* **95,** 063601 (2005).
56. Tran, T. T., Bray, K., Ford, M. J., Toth, M. & Aharonovich, I. Quantum emission from hexagonal boron nitride monolayers. *Nat. Nanotech.* **11,** 37–41 (2016).
57. He, Y.-M. *et al.* Single quantum emitters in monolayer semiconductors. *Nat. Nanotech.* **10,** 497–502 (2015).
58. Srivastava, A. *et al.* Optically active quantum dots in monolayer WSe_2. *Nat. Nanotech.* **10,** 491–496 (2015).
59. Kumar, S., Kaczmarczyk, A. & Gerardot, B. D. Strain-induced spatial and spectral isolation of quantum emitters in mono- and bilayer WSe_2. *Nano Lett.* **15,** 7567–7573 (2015).
60. Koperski, M. *et al.* Single photon emitters in exfoliated WSe_2 structures. *Nat. Nanotech.* **10,** 503–506 (2015).
61. Tonndorf, P. *et al.* Single-photon emission from localized excitons in an atomically thin semiconductor. *Optica* **2,** 347–352 (2015).
62. Chakraborty, C., Kinnischtzke, L., Goodfellow, K. M., Beams, R. & Vamivakas, A. N. Voltage-controlled quantum light from an atomically thin semiconductor. *Nat. Nanotech.* **10,** 507–511 (2015).

63. Kern, J. *et al.* Nanoscale positioning of single-photon emitters in atomically thin WSe_2. *Adv. Mater.* **28,** 7101–7105 (2016).
64. Bourrellier, R. *et al.* Bright UV single photon emission at point defects in h-BN. *Nano Lett.* **16,** 4317–4321 (2016).
65. Jungwirth, N. R. *et al.* Temperature dependence of wavelength selectable zero-phonon emission from single defects in hexagonal boron nitride. Preprint at http://arXiv.org/abs/1605.04445 (2016).
66. Martinez, L. J. *et al.* Efficient single photon emission from a high-purity hexagonal boron nitride crystal. Preprint at http://arXiv.org/abs/1606.04124 (2016).
67. Tran, T. T. *et al.* Quantum emission from defects in single-crystalline hexagonal boron nitride. *Phys. Rev. Appl.* **5,** 034005 (2016).
68. Ma, X., Hartmann, N. F., Baldwin, J. K. S., Doorn, S. K. & Htoon, H. Room-temperature single-photon generation from solitary dopants of carbon nanotubes. *Nat. Nanotech.* **10,** 671–675 (2015).
69. Hogele, A., Galland, C., Winger, M. & Imamoglu, A. Photon antibunching in the photoluminescence spectra of a single carbon nanotube. *Phys. Rev. Lett.* **100,** 217401 (2008).
70. Jeantet, A. *et al.* Widely tunable single-photon source from a carbon nanotube in the Purcell regime. *Phys. Rev. Lett.* **116,** 247402 (2016).
71. Akopian, N., Patriarche, G., Liu, L., Harmand, J. C. & Zwiller, V. Crystal phase quantum dots. *Nano Lett.* **10,** 1198–1201 (2010).
72. Dory, C. *et al.* Complete coherent control of a quantum dot strongly coupled to a nanocavity. *Sci. Rep.* **6,** 25172 (2016).
73. Sun, S., Kim, H., Solomon, G. S. & Waks, E. A quantum phase switch between a single solid-state spin and a photon. *Nat. Nanotech.* **11,** 539–544 (2016).
74. Santori, C., Pelton, M., Solomon, G., Dale, Y. & Yamamoto, Y. Triggered single photons from a quantum dot. *Phys. Rev. Lett.* **86,** 1502–1505 (2001).
75. Strauf, S. *et al.* High-frequency single-photon source with polarization control. *Nat. Photon.* **1,** 704–708 (2007).
76. Muller, M., Bounouar, S., Jons, K. D., Glässl, M. & Michler, P. On-demand generation of indistinguishable polarization-entangled photon pairs. *Nat. Photon.* **8,** 224–228 (2014).
77. Versteegh, M. A. M. *et al.* Observation of strongly entangled photon pairs from a nanowire quantum dot. *Nat. Commun.* **5,** 5298 (2014).
78. Stevenson, R. M. *et al.* Indistinguishable entangled photons generated by a light-emitting diode. *Phys. Rev. Lett.* **108,** 040503 (2012).
79. Gazzano, O. *et al.* Bright solid-state sources of indistinguishable single photons. *Nat. Commun.* **4,** 1425 (2013).
80. Claudon, J. *et al.* A highly efficient single-photon source based on a quantum dot in a photonic nanowire. *Nat. Photon.* **4,** 174–177 (2010).
81. Reimer, M. E. *et al.* Bright single-photon sources in bottom-up tailored nanowires. *Nat. Commun.* **3,** 737 (2012).
82. Munsch, M. *et al.* Dielectric GaAs antenna ensuring an efficient broadband coupling between an InAs quantum dot and a Gaussian optical beam. *Phys. Rev. Lett.* **110,** 177402 (2013).
83. Gschrey, M. *et al.* Highly indistinguishable photons from deterministic quantum-dot microlenses utilizing three-dimensional *in situ* electron-beam lithography. *Nat. Commun.* **6,** 7662 (2015).
84. Sapienza, L., Davanco, M., Badolato, A. & Srinivasan, K. Nanoscale optical positioning of single quantum dots for bright and pure single-photon emission. *Nat. Commun.* **6,** 7833 (2015).
85. Holmes, M. J., Choi, K., Kako, S., Arita, M. & Arakawa, Y. Room-temperature triggered single photon emission from a III-nitride site-controlled nanowire quantum dot. *Nano Lett.* **14,** 982–986 (2014).
86. Kako, S. *et al.* A gallium nitride single-photon source operating at 200 K. *Nat. Mater.* **5,** 887–892 (2006).
87. Deshpande, S., Das, A. & Bhattacharya, P. Blue single photon emission up to 200 K from an InGaN quantum dot in AlGaN nanowire. *Appl. Phys. Lett.* **102,** 161114 (2013).
88. Park, Y.-S., Guo, S., Makarov, N. S. & Klimov, V. I. Room temperature single-photon emission from individual perovskite quantum dots. *ACS Nano* **9,** 10386–10393 (2015).
89. Nowak, A. K. *et al.* Deterministic and electrically tunable bright single-photon source. *Nat. Commun.* **5,** 3240 (2014).
90. Shambat, G. *et al.* Ultrafast direct modulation of a single-mode photonic crystal nanocavity light-emitting diode. *Nat. Commun.* **2,** 539 (2011).
91. Reithmaier, G. *et al.* On-chip generation, routing, and detection of resonance fluorescence. *Nano Lett.* **15,** 5208–5213 (2015).
92. Murray, E. *et al.* Quantum photonics hybrid integration platform. *Appl. Phys. Lett.* **107,** 171108 (2015).
93. Arcari, M. *et al.* Near-unity coupling efficiency of a quantum emitter to a photonic crystal waveguide. *Phys. Rev. Lett.* **113,** 093603 (2014).
94. Heindel, T. *et al.* Electrically driven quantum dot-micropillar single photon source with 34% overall efficiency. *Appl. Phys. Lett.* **96,** 011107 (2010).
95. Deshpande, S., Heo, J., Das, A. & Bhattacharya, P. Electrically driven polarized single-photon emission from an InGaN quantum dot in a GaN nanowire. *Nat. Commun.* **4,** 1675 (2013).
96. Palacios-Berraquero, C. *et al.* Atomically thin quantum light-emitting diodes. *Nat. Commun.* **7,** 12978 (2016).
97. Clark, G. *et al.* Single defect light-emitting diode in a van der Waals heterostructure. *Nano Lett.* **16,** 3944–3948 (2016).
98. Mizuochi, N. *et al.* Electrically driven single-photon source at room temperature in diamond. *Nat. Photon.* **6,** 299–303 (2012).
99. Lohrmann, A. *et al.* Diamond based light-emitting diode for visible single-photon emission at room temperature. *Appl. Phys. Lett.* **99,** 251106 (2012).
100. Salter, C. L. *et al.* An entangled-light-emitting diode. *Nature* **465,** 594–597 (2010).
101. Zaitsev, A. M., Bergman, A. A., Gorokhovsky, A. A. & Huang, M. B. Diamond light emitting diode activated with Xe optical centers. *Phys. Status Solidi A* **203,** 638–642 (2006).
102. Berhane, A. M. *et al.* Electrical excitation of silicon-vacancy centers in single crystal diamond. *Appl. Phys. Lett.* **106,** 171102 (2015).
103. Wong, D. *et al.* Characterization and manipulation of individual defects in insulating hexagonal boron nitride using scanning tunnelling microscopy. *Nat. Nanotech.* **10,** 949–953 (2015).
104. Pelton, M. Modified spontaneous emission in nanophotonic structures. *Nat. Photon.* **9,** 427–435 (2015).
105. Benson, O. Assembly of hybrid photonic architectures from nanophotonic constituents. *Nature* **480,** 193–199 (2011).
106. Englund, D. *et al.* Deterministic coupling of a single nitrogen vacancy center to a photonic crystal cavity. *Nano Lett.* **10,** 3922–3926 (2010).
107. Kolchin, P. *et al.* High Purcell factor due to coupling of a single emitter to a dielectric slot waveguide. *Nano Lett.* **15,** 464–468 (2015).
108. Hoang, T. B., Akselrod, G. M. & Mikkelsen, M. H. Ultrafast room-temperature single photon emission from quantum dots coupled to plasmonic nanocavities. *Nano Lett.* **16,** 270–275 (2016).
109. Miura, R. *et al.* Ultralow mode-volume photonic crystal nanobeam cavities for high-efficiency coupling to individual carbon nanotube emitters. *Nat. Commun.* **5,** 5580 (2014).
110. Yalla, R., Sadgrove, M., Nayak, K. P. & Hakuta, K. Cavity quantum electrodynamics on a nanofiber using a composite photonic crystal cavity. *Phys. Rev. Lett.* **113,** 143601 (2014).
111. Albrecht, R., Bommer, A., Deutsch, C., Reichel, J. & Becher, C. Coupling of a single nitrogen-vacancy center in diamond to a fiber-based microcavity. *Phys. Rev. Lett.* **110,** 243602 (2013).
112. Liu, X. *et al.* Strong light–matter coupling in two-dimensional atomic crystals. *Nat. Photon.* **9,** 30–34 (2015).
113. Schmitt-Manderbach, T. *et al.* Experimental demonstration of free-space decoy-state quantum key distribution over 144 km. *Phys. Rev. Lett.* **98,** 010504 (2007).
114. Lo, H. K., Ma, X. F. & Chen, K. Decoy state quantum key distribution. *Phys. Rev. Lett.* **94,** 230504 (2005).
115. Takemoto, K. *et al.* Quantum key distribution over 120 km using ultrahigh purity single-photon source and superconducting single-photon detectors. *Sci. Rep.* **5,** 14383 (2015).
116. Guha, S. *et al.* Rate-loss analysis of an efficient quantum repeater architecture. *Phys. Rev. A* **92,** 022357 (2015).
117. Azuma, K., Tamaki, K. & Lo, H.-K. All-photonic quantum repeaters. *Nat. Commun.* **6,** 6787 (2015).
118. Pant, M., Krovi, H., Englund, D. & Guha, S. Rate-distance tradeoff and resource costs for all-optical quantum repeaters. Preprint at https://arXiv.org/abs/1603.01353 (2016).
119. Li, Y., Humphreys, P. C., Mendoza, G. J. & Benjamin, S. C. Resource costs for fault-tolerant linear optical quantum computing. *Phys. Rev. X* **5,** 041007 (2015).
120. Peruzzo, A. *et al.* Quantum walks of correlated photons. *Science* **329,** 1500–1503 (2010).
121. Rohde, P. P. Boson sampling with photons of arbitrary spectral structure. *Phys. Rev. A* **91,** 012307 (2015).
122. He, Y.-M. *et al.* On-demand semiconductor single-photon source with near-unity indistinguishability. *Nat. Nanotech.* **8,** 213–217 (2013).
123. Nilsson, J. *et al.* Quantum teleportation using a light-emitting diode. *Nat. Photon.* **7,** 311–315 (2013).
124. Rondin, L. *et al.* Magnetometry with nitrogen-vacancy defects in diamond. *Rep. Prog. Phys.* **77,** 056503 (2014).
125. Bernien, H. *et al.* Heralded entanglement between solid-state qubits separated by three metres. *Nature* **497,** 86–90 (2013).
126. Aspelmeyer, M., Kippenberg, T. J. & Marquardt, F. Cavity optomechanics. *Rev. Mod. Phys.* **86,** 1391–1452 (2014).

127. Yeo, I. *et al.* Strain-mediated coupling in a quantum dot-mechanical oscillator hybrid system. *Nat. Nanotech.* **9,** 106–110 (2014).
128. Teissier, J., Barfuss, A., Appel, P., Neu, E. & Maletinsky, P. Strain coupling of a nitrogen-vacancy center spin to a diamond mechanical oscillator. *Phys. Rev. Lett.* **113,** 020503 (2014).
129. Ovartchaiyapong, P., Lee, K. W., Myers, B. A. & Jayich, A. C. B. Dynamic strain-mediated coupling of a single diamond spin to a mechanical resonator. *Nat. Commun.* **5,** 4429 (2014).
130. Khanaliloo, B. *et al.* Single-crystal diamond nanobeam waveguide optomechanics. *Phys. Rev. X* **5,** 041051 (2015).
131. MacQuarrie, E. R., Gosavi, T. A., Jungwirth, N. R., Bhave, S. A. & Fuchs, G. D. Mechanical spin control of nitrogen-vacancy centers in diamond. *Phys. Rev. Lett.* **111,** 227602 (2013).
132. Burek, M. J. *et al.* Diamond optomechanical crystals. Preprint at http://arXiv.org/abs/1512.04166 (2016).
133. Bracher, D. O. & Hu, E. L. Fabrication of high-*Q* nanobeam photonic crystals in epitaxially grown 4H-SiC. *Nano Lett.* **15,** 6202–6207 (2015).
134. Tiarks, D., Baur, S., Schneider, K., Dürr, S. & Rempe, G. Single-photon transistor using a Förster resonance. *Phys. Rev. Lett.* **113,** 053602 (2014).
135. Hwang, J. *et al.* A single-molecule optical transistor. *Nature* **460,** 76–80 (2009).
136. Fuechsle, M. *et al.* A single-atom transistor. *Nat. Nanotech.* **7,** 242–246 (2012).
137. Shomroni, I. *et al.* All-optical routing of single photons by a one-atom switch controlled by a single photon. *Science* **345,** 903–906 (2014).
138. Neu, E. *et al.* Single photon emission from silicon-vacancy centres in CVD-nano-diamonds on iridium. *New J. Phys.* **13,** 025012 (2011).
139. Schröder, T., Gädeke, F., Banholzer, M. J. & Benson, O. Ultrabright and efficient single-photon generation based on nitrogen-vacancy centres in nanodiamonds on a solid immersion lens. *New J. Phys.* **13,** 055017 (2011).
140. Siyushev, P. *et al.* Low-temperature optical characterization of a near-infrared single-photon emitter in nanodiamonds. *New J. Phys.* **11,** 113029 (2009).
141. Siyushev, P. *et al.* Coherent properties of single rare-earth spin qubits. *Nat. Commun.* **5,** 3895 (2014).
142. Luozhou, L. *et al.* Efficient photon collection from a nitrogen vacancy center in a circular bullseye grating. *Nano Lett.* **15,** 1493–1497 (2015).

Acknowledgements

We thank C.-Y. Lu for discussions, and G. Fuchs, P. Barclay, D. Lake, R. Johne and A. Fiore for assistance with images. Financial support from the Australian Research Council (via DP140102721, IH150100028, DE130100592), FEI Company, the Asian Office of Aerospace Research and Development grant FA2386-15-1-4044, the Army Research Laboratory, the Center for Distributed Quantum Information program and the Air Force Office of Scientific Research Multidisciplinary University Research Initiative (FA9550-14-1-0052) is gratefully acknowledged.

Additional information

Reprints and permissions information is available online at www.nature.com/reprints.
Correspondence should be addressed to I.A.

Competing financial interests

The authors declare no competing financial interests.